ISSN: 1410-8917
Jurnal Kimia Sains & Aplikasi
e-ISSN: 2597-9914

Jurnal Kimia Sains dan Aplikasi 29 (5) (2026): 373-378

Jurnal Kimia Sains dan Aplikasi
Journal of Scientific and Applied Chemistry

Journal homepage: http://ejournal.undip.ac.id/index.php/ksa

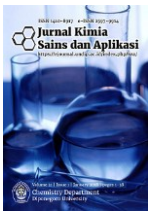

The Release of Curcumin from β-TCP/SiO_2/Curcumin Composites in a Ringer's Lactate Solution

Tri Windarti *, Ngadiwiyana, Fadila Fibriani

Chemistry Department, Faculty of Sciences and Mathematics, Universitas Diponegoro, Jl. Prof. Soedarto S.H, Tembalang, Semarang 50275, Indonesia

* Corresponding author: tri.windarti@live.undip.ac.id

https://doi.org/10.14710/jksa.29.5.373-378

Article Info

Article history:

Received: 08th April 2026
Revised: 05th June 2026
Accepted: 10th June 2026
Online: 15th June 2026

Keywords:
Calcium phosphate cement; β- TCP; SiO_2; curcumin

Abstract

Osteoporosis is characterized by bone deterioration caused by high levels of reactive oxygen species (ROS), which inhibit osteoblast activity and lead to a decrease in bone density. Adding curcumin, a natural antioxidant, to calcium phosphate cement (CPC) enhances its function beyond simply increasing bone density. In this study, CPC was prepared from a β-tricalcium phosphate (β-TCP, β-$Ca_3(PO_4)_2$) composite with curcumin. To enhance the interaction between β- TCP and curcumin, silicon dioxide (SiO_2) was added. β-TCP was synthesized by the sol-gel method, with SiO_2 content ranging from 1.6 to 8.3%. CPC preparation was carried out using a 2.5% Na_2HPO_4 solution. The release of curcumin in a Ringer's lactate solution was studied in relation to the role of SiO_2. The UV-Vis spectral intensity of the remaining Ringer's lactate solution after soaking decreased as the SiO_2 content increased. Results from a five-day soaking period showed that β-TCP did not transform into hydroxyapatite, but rather experienced a decrease in crystallinity and average crystal size from 96.175% to 25.524% and from 58.335 nm to 39.474 nm, respectively. Therefore, it can be predicted that CPC can maintain the presence of curcumin in a physiological environment.

1. Introduction

Bones are an essential component of the human body. They are primarily composed of minerals, such as calcium and phosphorus, as well as organic components, such as collagen [1]. Bones can become damaged with age [2]. Osteoporosis, a common bone condition among the elderly, is characterised by a decrease in bone density that leads to reduced bone strength and an increased risk of fractures. This decrease in bone density is caused by increased osteoclast activity relative to osteoblast activity [3]. Osteoclast and osteoblast activity is imbalanced due to oxidative stress resulting from high levels of reactive oxygen species (ROS) [4]. Osteoporosis-related fractures can be prevented using calcium phosphate cement (CPC) injections. This substance breaks down in the body to release calcium and phosphate ions, which stimulate the formation of new bone tissue [5].

One calcium phosphate compound developed for use as a bone cement is β-tricalcium phosphate (β-TCP, or β-$Ca_3(PO_4)_2$). It has a Ca/P molar ratio of 1.5 and a rhombohedral crystal structure [6]. This compound is biocompatible, osteoconductive, and biodegradable [7, 8]. β-TCP can be synthesized using several methods, such as hydrothermal, microemulsion, and sol-gel. The sol- gel method is widely used because it can produce high-purity β-TCP, as demonstrated by [9].

In the treatment of osteoporosis, compounds with antioxidant properties are needed to reduce high levels of ROS. ROS are reactive oxygen species that consist of various molecules, one of which is superoxide (O_2^-). Superoxide is a ROS because it has an unpaired electron, which makes it highly reactive. Antioxidant compounds can interact directly with ROS, reducing their levels [4]. Curcumin ($C_{21}H_{20}O_6$) is a polyphenolic compound with antioxidant properties that can minimize the effects of oxidative stress [10]. To prepare CPC based on β-TCP and curcumin, a binder is required to connect the components, and SiO_2 is suitable for this purpose [11]. The presence of SiO_2 in calcium phosphate cement increases the surface's electronegativity, thereby promoting new bone formation [12]. Hashimoto et al. have researched

β- TCP/SiO_2 composites. The addition of SiO_2 to these composites can increase their mechanical strength and density while reducing porosity.

The amount of SiO_2 incorporated into the composite is expected to influence the number of silanol (Si–OH) groups available to interact with both curcumin and β- TCP. These interactions may affect the release behavior of curcumin when the composite is exposed to physiological fluids. Curcumin release is thought to be regulated through hydrogen bonding and electrostatic interactions. Therefore, this study aimed to investigate the effect of SiO_2 content on the release behavior of curcumin from β-TCP/SiO_2/curcumin composites in Ringer's lactate solution. β-TCP was synthesized via the sol–gel method using cetyltrimethylammonium bromide (CTAB) as a morphology-directing agent. Curcumin release was analyzed using UV–Vis spectrophotometry, while structural and morphological changes before and after immersion were characterized by Fourier-transform infrared spectroscopy (FTIR), X-ray diffraction (XRD), and field-emission scanning electron microscopy coupled with energy-dispersive X-ray spectroscopy (FE-SEM/EDX).

2. Experimental

2.1. Materials

The chemicals used in this study were calcium nitrate tetrahydrate ($Ca(NO_3)_2{\cdot}4H_2O$, Merck), potassium dihydrogen phosphate (KH_2PO_4, Merck), cetyltrimethylammonium bromide (CTAB, Sigma-Aldrich), ammonium hydroxide (NH_4OH, 32%, Merck), curcumin (Merck), silicon dioxide (SiO_2, Merck), disodium hydrogen phosphate (Na_2HPO_4, Merck), and Ringer's lactate solution (Otsuka).

2.2. Instruments

The instruments used in this study included a Fourier Transform Infrared (FTIR) spectrometer (Bruker), an X- ray diffractometer (XRD, Rigaku), a Field Emission Scanning Electron Microscope equipped with Energy-Dispersive X-ray Spectroscopy (FE-SEM/EDX, JSM-IT), and a UV–Vis spectrophotometer (Shimadzu).

2.3. Experimental Procedures

2.3.1. Synthesis of β-TCP

Beta-TCP was synthesised using the sol-gel method. A calcium solution was prepared by dissolving 14.160 g of $Ca(NO_3)_2{\cdot}4H_2O$ and 0.0164 g of CTAB in distilled water, yielding 50 mL of solution. Similarly, the phosphate solution was prepared by dissolving 6.804 g of KH_2PO_4 and 0.0164 g of CTAB in distilled water, yielding a final volume of 50 mL. The calcium solution was then slowly added to the phosphate solution, stirred with a magnetic stirrer. Next, 15 mL of 32% ammonium hydroxide solution was added until the pH value exceeded 9. The solution was stirred for 1 hour, after which it was aged for 48 hours. After aging, the precipitate was washed with distilled water until the pH reached neutrality. The precipitate was dried in an oven at 40°C for 48 hours. This was then calcined at 800°C for 30 minutes. Finally, the calcined powder was sieved using a 100-mesh sieve.

Table 1. Sample codes and composite composition

Sample code	β-TCP (g)	Curcumin (g)	SiO_2 (g)	SiO_2 content (%)
K1	2.80	0.15	0.05	1.6
K2	2.75	0.15	0.10	3.3
K3	2.70	0.15	0.15	5.0
K4	2.65	0.15	0.20	6.6
K5	2.60	0.15	0.25	8.3

2.3.2. Preparation of β-TCP/SiO_2/Curcumin Composites

The composite was prepared using powdered components consisting of a mixture of β-TCP, SiO_2, and curcumin, according to the composition shown in Table 1. A 2.5% Na_2HPO_4 solution was used as the liquid component. The powdered components were first homogenised using a spatula, and then mixed with the Na_2HPO_4 solution. The mixture was stirred with a spatula until a homogeneous paste formed. The volume of the 2.5% Na_2HPO_4 solution required was recorded in order to determine the liquid-to-powder ratio. The paste was then placed in moulds measuring 0.5 cm in height and 1.5 cm in diameter, after which it was left to dry at room temperature.

2.3.3. Curcumin Release Test

The samples were immersed in 100 mL of Ringer's lactate solution for five days. The release profile of curcumin from the composite was then tested using a UV- Vis spectrophotometer.

2.3.4. Characterization of β-TCP and β-TCP/SiO_2/Curcumin Composites

The success of the synthesis was assessed by identifying the diffraction peaks formed using XRD instruments to characterise the β-TCP. The β- TCP/SiO_2/curcumin composite, which had been immersed in Ringer's lactate solution, was characterised using FTIR, XRD, and FE-SEM/EDX instruments. These instruments were used to determine the structural and morphological changes that occurred in the composite after a 5-day immersion process.

3. Results and Discussion

The synthesis of β-TCP yielded a white powder with an average weight of 5.759 g. Figure 1 shows the XRD pattern of β-TCP, scanned over 2θ = 5–60°. The refinement results indicate the presence of β-TCP, represented by the blue line, and hydroxyapatite ($Ca_{10}(PO_4)_6(OH)_2$), represented by the green line. High-intensity diffraction peaks appear at 2θ = 31.231°, 34.459°, and 27.936°. These correspond to the XRD patterns of the (0 2 10), (2 2 0), and (2 1 4) planes of β-TCP, respectively [13]. These peaks correspond to JCPDS data no. 09-0169 for β-TCP. The synthesised β-TCP consists of 97.8% β- TCP and 2.2% hydroxyapatite (HA). Given this composition, the product can be said 97.8% pure β-TCP. It has a crystallinity of 96% and an average crystal size of 58 nm.

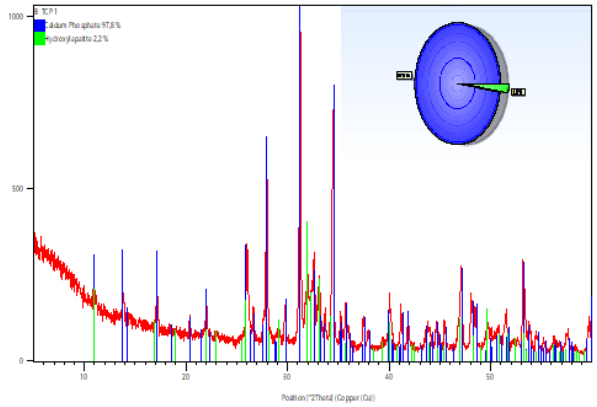

Figure 1. XRD diffractogram of synthesised β-TCP, including refinement result

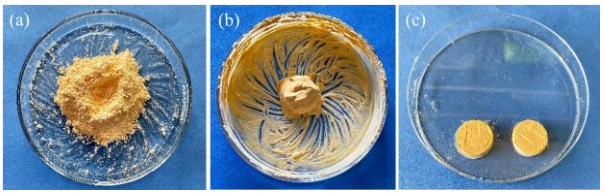

Figure 2. CPC preparation: powder components (a), paste (b), and CPC molding (c)

The synthesised β-TCP was then used as the main ingredient in preparing CPC. This was achieved by combining powdered components, consisting of β-TCP, curcumin, and SiO_2, with a liquid component in the form of a 2.5% Na_2HPO_4 solution (Figure 2a). The powder and liquid components were mixed and stirred with a spatula. The required volume of liquid component varies: 2.5 mL of a 2.5% Na_2HPO_4 solution was required for samples K1 and K2, 2.7 mL for sample K3, 2.9 mL for sample K4, and 2.8 mL for sample K5. It can be said that the required volume of the liquid component tends to increase as the amount of SiO_2 used increases. The mixing process continued until a homogeneous paste was formed (Figure 2b). This paste was then moulded into a mould with dimensions of 0.5 cm in height and 1.5 cm in diameter and was then left to dry at room temperature (Figure 2c). Figure 3 shows the appearance of the samples after drying, with a CPC weight ranging from 0.9 to 1 g.

The dried CPC was then immersed in 100 mL of Ringer's lactate solution for five days. Because its composition and pH resemble human body fluids, Ringer's lactate is a relevant medium for evaluating CPC behavior [14]. Composites of β-TCP/SiO_2/curcumin with varying SiO_2 content (1.6–8.3%) were immersed in 100 mL of Ringer's lactate solution for five days. Visual observation showed CPC formation after immersion, and higher SiO_2 content reduced sample disintegration (Figure 4a). The Ringer's lactate solution turned from clear to yellowish, indicating curcumin release (Figure 4b). A similar behavior has been reported for hydroxyapatite/SiO_2/curcumin composites in Ringer's lactate solution [15].

Curcumin release begins with water diffusion from Ringer's lactate into the CPC, weakening interactions between β-TCP and curcumin mediated by silanol (Si–OH) groups in SiO_2. Continued water diffusion then causes the CPC to disintegrate. It was found that the disintegration decreased as the SiO_2 content increased. This is evident from the UV-Vis absorbance values measured in the Ringer's lactate solution after soaking. As the SiO_2 concentration increased, the absorbance at 200–600 nm tended to decrease (Figure 5). Curcumin's resistance to leaching from CPC is attributed to its bonding with silanol groups. All samples exhibited a peak at 212 nm. This differs from the absorption value of pure curcumin at pH 7.4, which is 420 nm [16]. The observed peaks result from the interaction between curcumin, β- TCP and SiO_2, as well as the Ringer's lactate solution. Additionally, an n → π* electronic transition from the diketone group in curcumin can produce a peak at a wavelength of around 200 nm [17].

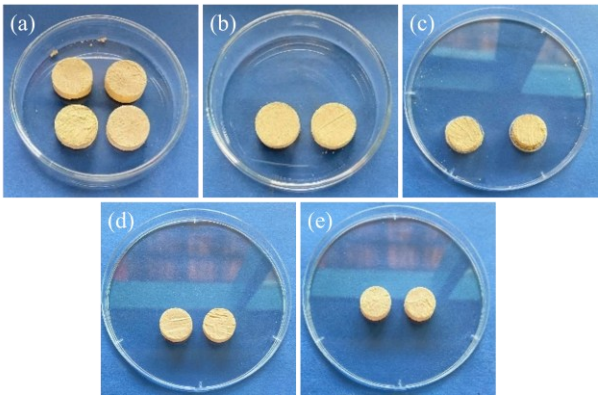

Figure 3. The appearance of dried CPC for samples K1 (a), K2 (b), K3 (c), K4 (d), and K5 (e)

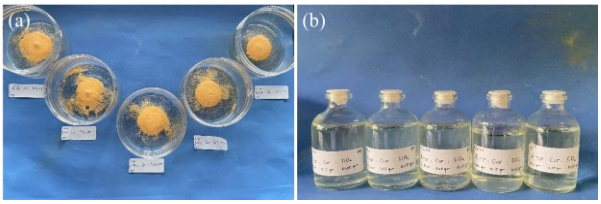

Figure 4. CPC after immersion in Ringer's lactate solution (a) and the remaining Ringer's lactate solution after immersion (b)

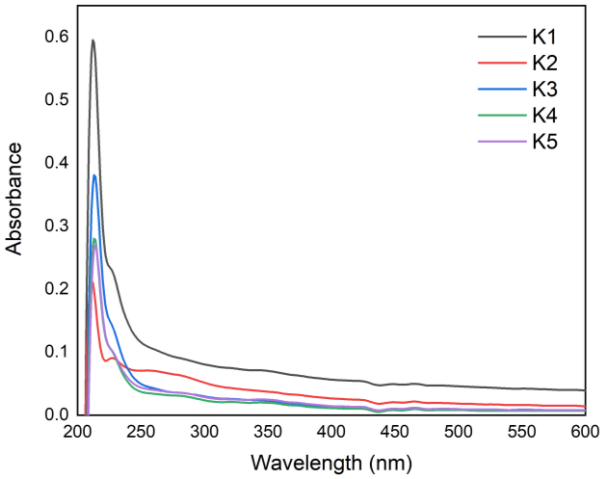

Figure 5. UV-Vis spectra of the Ringer's lactate solution remaining after soaking

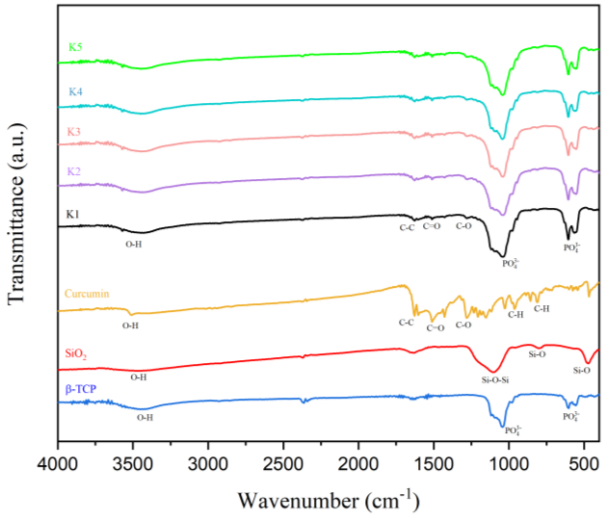

Figure 6. FTIR spectra of CPC after immersion in Ringer's lactate solution

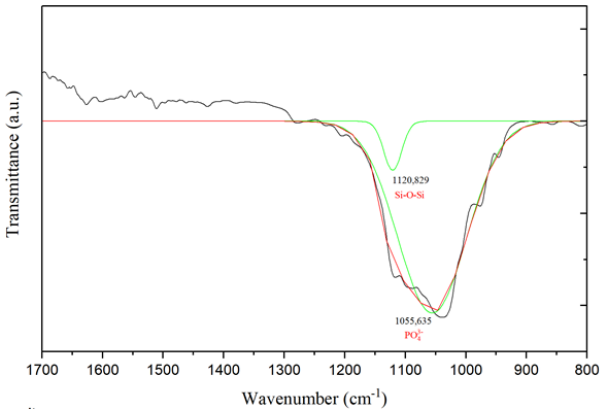

Figure 7. Deconvolution of the PO_4^{3-} peak

CPC samples that had been soaked in a Ringer's lactate solution were characterised using an FTIR instrument (Figure 6). This was done to determine the structural changes that occurred after soaking. The spectra of all samples exhibited a consistent pattern, revealing the presence of β-TCP, SiO_2, and curcumin. The stretching and bending vibrations of the PO_4^{3-} group appeared at wavenumbers of 604, 554, and 1038 cm^{-1} [11]. The presence of curcumin can be demonstrated by the O– H stretching vibration at a wavenumber of 3449 cm^{-1} [15]; C–C stretching vibrations at 1626 cm^{-1}; C–O stretching vibrations at 1279 cm^{-1} [16]; and C=O vibrations at a wavenumber of 1510 cm^{-1} [18]. The Si-O-Si vibration overlaps with the PO_4^{3-} peak. This causes the PO_4^{3-} peak to broaden. Figure 7 shows the deconvoluted PO_4^{3-} peak, in which the PO_4^{3-} stretching vibration appears at a wavenumber of 1056 cm^{-1} and the Si-O-Si vibration at 1121 cm^{-1}. The shift in the wavenumbers of the Si-O-Si and PO_4^{3-} vibrations from 1103 and 1042 cm^{-1} to 1121 and 1056 cm^{-1}, respectively, occurs due to interactions between silica, β-TCP, and curcumin [15].

An XRD analysis was performed on sample K1 after it had been immersed in a Ringer's lactate solution, in order to determine any changes in diffraction patterns, crystallinity, and crystal size (Figure 8). Several peaks characteristic of curcumin appeared at 2θ = 10–25° [19]. The characteristic peaks of β-TCP can clearly be seen in the diffractogram at 2θ = 27.820°, 31.111°, and 34.373°. The 2θ values of β-TCP in sample K1 shifted slightly towards smaller values after soaking. Sample K1's crystallinity decreased to 26%, compared to 96% for β-TCP. The average crystal size of sample K1 was 39 nm, which is smaller than the 58 nm average for β-TCP. The decrease in crystallinity and crystal size was caused by water diffusing from the Ringer's lactate solution into the CPC.

FE-SEM/EDX analysis was performed on sample K1 to determine its morphology and the distribution of its constituent elements following a 5-day immersion in Ringer's lactate solution. Figure 9 shows FE-SEM images of sample K1 at magnifications of 5,000, 10,000, 25,000, and 50,000 times. At 5,000× magnification, clumps with surfaces made up of small particles become visible. Increasing the magnification to 10,000× reveals an uneven surface and the presence of voids. At 25,000× magnification, three particle sizes are visible: large, medium, and small. At 50,000× magnification, the shape and size of the particles can be confirmed: irregularly shaped particles smaller than 100 nm agglomerate to form larger particles. This agglomeration creates interparticle spaces, resulting in voids. CPC with these characteristics is highly desirable because the voids allow bone cells to proliferate and enable bone remodelling [20, 21, 22].

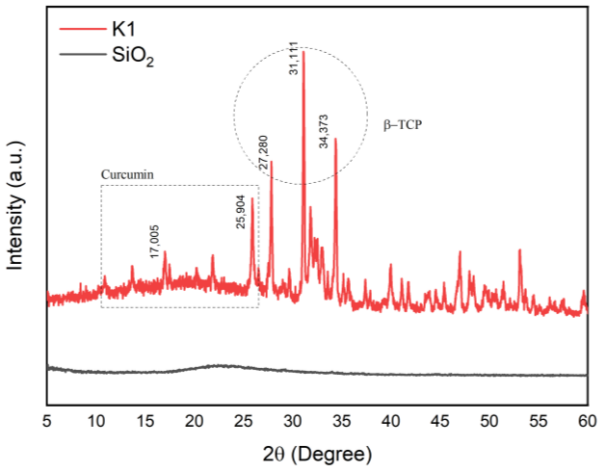

Figure 8. XRD diffractogram of sample K1

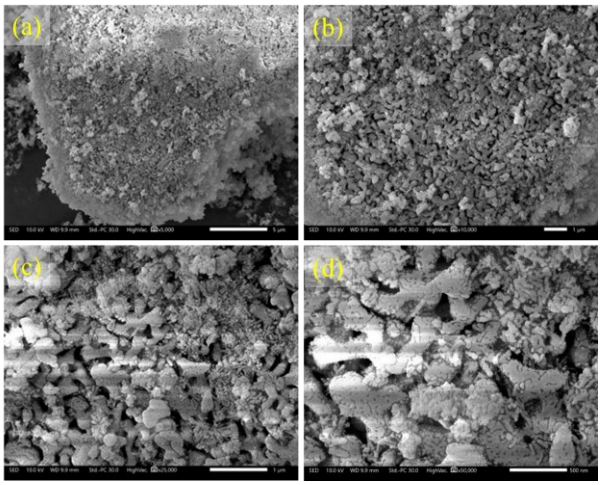

Figure 9. FE-SEM images of sample K1 at magnifications of 5,000× (a), 10,000× (b), 25,000× (c), and 50,000× (d)

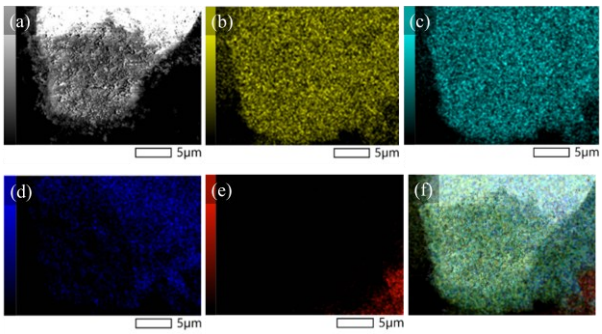

Figure 10. Elemental mapping of sample K1; mapping area (a), Ca (b), P (c), (O) (d), C (e), and combination of elements (f)

Table 2. Element composition of the surface of sample K1

Element	%
O	51.52 ± 0.64
Ca	24.65 ± 0.38
P	15.76 ± 0.23
C	8.08 ± 0.19
Ca/P	1.56

Figure 10a shows the elemental mapping of the surface of the K1 sample. Mapping was performed for the elements calcium (Ca), phosphorus (P), oxygen (O), and carbon (C) (Figures 10b–10e). The results showed that the surface of sample K1 is dominated by Ca, P, and O, which indicates the presence of β-TCP. The presence of curcumin is represented by the elements C and O, which are located separately. This suggests that the composite is not homogeneous, possibly because the non-polar nature of curcumin leads it to interact indirectly with the calcium phosphate surface via the silanol groups on SiO_2. The results of the combined element mapping are shown in Figure 10f. The Ca- and P-rich surface of CPC ensures that the superior properties of β-TCP are maintained while it remains in the physiological environment.

Table 2 shows the percentage of elements on the surface of sample K1. The element O dominates the surface because oxygen is present in β-TCP, SiO_2, and curcumin. By ignoring the existence of silicon (Si), the number of oxygen atoms = 51.52 %, Ca = 24.65 %, P = 15.76 %, and C = 8.08 %. This composition yields a Ca/P molar ratio of 1.56, close to the β-TCP value of 1.5. It can be concluded that immersing the CPC in Ringer's lactate solution for five days did not result in the transformation of β-TCP into hydroxyapatite.

4. Conclusion

The sol-gel synthesis method produced β-TCP with a purity of 97.8%. CPC was formed through the interaction between β-TCP and curcumin, mediated by the silanol (OH) group. As the SiO_2 content increased, the amount of curcumin released into the Ringer's lactate solution decreased. After five days of immersion, β-TCP did not transform into hydroxyapatite but exhibited a decrease in crystallinity from 96.175% to 25.524% and a reduction in crystallite size from 58.335 nm to 39.474 nm as a result of water diffusion into the composite. These findings suggest that the β-TCP/SiO_2/curcumin composite has the potential to sustain the presence of curcumin under physiological conditions. Further studies are required to evaluate the antioxidant activity and stability of released curcumin following immersion in Ringer's lactate solution.

Acknowledgement

We would like to thank the Physical Chemistry Laboratory at Diponegoro University for providing us with the necessary research facilities.

References

[1] Veronika Šromová, Dinara Sobola, Pavel Kaspar, A Brief Review of Bone Cell Function and Importance, *Cells*, 12, 21, (2023), 2576 https://doi.org/10.3390/cells12212576

[2] Anjarsari Anjarsari, Kiagus Dahlan, Pipih Suptijah, Tetty Kemala, Synthesis and Characterization of Biocomposite BCP/Collagen for Bone Material Scaffold, *Jurnal Pengolahan Hasil Perikanan Indonesia*, 19, 3, (2016), 356-361

[3] Xiao Liang, Xindi Yang, Jing Liu, Lingfeng Tu, Wenxiang Wei, Hanjian Wang, Minhao Wu, Lin Cai, Yong Zheng, Yun Chen, ROS-scavenging bioactive scaffold orchestrates bone regeneration for osteoporotic bone defect repair, *Composites Part B: Engineering*, 281, (2024), 111528 https://doi.org/10.1016/j.compositesb.2024.111528

[4] Vladana Domazetovic, Gemma Marcucci, Teresa Iantomasi, Maria Luisa Brandi, Maria Teresa Vincenzini, Oxidative stress in bone remodeling: Role of antioxidants, *Clinical Cases in Mineral and Bone Metabolism*, 14, 2, (2017), 209-216

[5] Dhrumi Patel, Sarika Wairkar, Bone regeneration in osteoporosis: opportunities and challenges, *Drug Delivery and Translational Research*, 13, 2, (2023), 419-432 https://doi.org/10.1007/s13346-022-01222-6

[6] Jiwoon Jeong, Jung Hun Kim, Jung Hee Shim, Nathaniel S. Hwang, Chan Yeong Heo, Bioactive calcium phosphate materials and applications in bone regeneration, *Biomaterials Research*, 23, 1, (2019), s40824-40018-40149-40823 https://doi.org/10.1186/s40824-018-0149-3

[7] Chao Pan, Xiaohao Sun, Guangquan Xu, Yue Su, Debao Liu, The effects of β-TCP on mechanical properties, corrosion behavior and biocompatibility of β-TCP/Zn-Mg composites, *Materials Science and Engineering C*, 108, (2020), 110397 https://doi.org/10.1016/j.msec.2019.110397

[8] Dongxu Ke, Solaiman Tarafder, Sahar Vahabzadeh, Susmita Bose, Effects of MgO, ZnO, SrO, and SiO_2 in tricalcium phosphate scaffolds on *in vitro* gene expression and *in vivo* osteogenesis, *Materials Science and Engineering C*, 96, (2019), 10-19 https://doi.org/10.1016/j.msec.2018.10.073

[9] K. P. Sanosh, M. C. Chu, A. Balakrishnan, T. N. Kim, S. J. Cho, Sol-gel synthesis of pure nano sized β-tricalcium phosphate crystalline powders, *Current Applied Physics*, 10, 1, (2010), 68-71 https://doi.org/10.1016/j.cap.2009.04.014

[10] Karolina Jakubczyk, Aleksandra Drużga, Janda Katarzyna, Karolina Skonieczna-Żydecka, Antioxidant Potential of Curcumin—A Meta-Analysis of Randomized Clinical Trials, *Antioxidants*, 9, 11, (2020), 1-13 https://doi.org/10.3390/antiox9111092

[11] Kazuaki Hashimoto, Masahiko Oiwa, Hirobumi Shibata, Effect of Silicon Dioxide Nanoparticles on the Sintering Properties of Beta-Tricalcium Phosphate Composites, *Materials*, 17, 4, (2024), 797 https://doi.org/10.3390/ma17040797

[12] Charles T. Price, Kenneth J. Koval, Joshua R. Langford, Silicon: A Review of Its Potential Role in the Prevention and Treatment of Postmenopausal Osteoporosis, *International Journal of Endocrinology*, 2013, 1, (2013), 316783 https://doi.org/10.1155/2013/316783

[13] Tri Windarti, Limpat Nulandaya, Widjijono Widjijono, Nuryono Nuryono, Synthesis and Characterization of Biphasic Calcium Phosphate Substituted Cerium as a Potential Osteoporotic Bone Filler, *Periodica Polytechnica Chemical Engineering*, 67, 2, (2023), 242-255 https://doi.org/10.3311/PPch.21111

[14] Julian L. Seifter, Integration of Acid–Base and Electrolyte Disorders, *New England Journal of Medicine*, 371, (2014), 1821-1831 https://doi.org/10.1056/NEJMra1215672

[15] Tri Windarti, Nor Basid Adiwibawa Prasetya, Ngadiwiyana Ngadiwiyana, The Effect of SiO_2 Addition to the Hydroxyapatite/Curcumin Composite Properties, *Indonesian Journal of Chemistry*, 24, 5, (2024), 1361-1376 https://doi.org/10.22146/ijc.93802

[16] María L. Del Prado-Audelo, Isaac H. Caballero-Florán, Jorge A. Meza-Toledo, Néstor Mendoza-Muñoz, Maykel González-Torres, Benjamín Florán, Hernán Cortés, Gerardo Leyva-Gómez, Formulations of Curcumin Nanoparticles for Brain Diseases, *Biomolecules*, 9, 2, (2019), 56 https://doi.org/10.3390/biom9020056

[17] Susila Kristianingrum, *Handout Spektroskopi Ultra Violet dan Sinar Tampak (Spektroskopi UV-Vis)*, Universitas Negeri Yogyakarta, Yogyakarta, 2013

[18] Vignesh Krishnan, G. Devanand Venkatasubbu, T. Kalaivani, Investigation of hemolysis and antibacterial analysis of curcumin-loaded mesoporous SiO_2 nanoparticles, *Applied Nanoscience*, 13, (2023), 811-818 https://doi.org/10.1007/s13204-021-01910-8

[19] Zahra Sayyar, Hoda Jafarizadeh Malmiri, Photocatalytic and antibacterial activities study of prepared self-cleaning nanostructure surfaces using synthesized and coated ZnO nanoparticles with Curcumin nanodispersion, *Zeitschrift für Kristallographie - Crystalline Materials*, 234, 5, (2019), 307-328 https://doi.org/10.1515/zkri-2018-2096

[20] Monikaq Bielec, An Huang, Yuhao Xia, Honglian Dai, Microemulsion Synthesis of Mesoporous β-tricalcium Phosphate Powder with a Novel System, *Journal of Wuhan University of Technology-Materials Science Edition*, 37, (2022), 773-778 https://doi.org/10.1007/s11595-022-2595-y

[21] Nashaat N. Nassar, Stefania Betancur, Sócrates Acevedo, Camilo A. Franco, Farid B. Cortés, Development of a Population Balance Model to Describe the Influence of Shear and Nanoparticles on the Aggregation and Fragmentation of Asphaltene Aggregates, *Industrial and Engineering Chemistry Research*, 54, 33, (2015), 8201-8211 https://doi.org/10.1021/acs.iecr.5b02075

[22] Katherine Kho, Denny Nugroho, Asaf Kleopas Sugih, Preparation and Characterization of Highly Water Soluble Curcumin–Dextrose Cocrystal, *Journal of Pure and Applied Chemistry Research*, 7, 2, (2018), 139-147 https://doi.org/10.21776/ub.jpacr.2018.007.02.401